J. Woisetschläger, R. Pecnik, E.Göttlich, O.Schennach, A.Marn, W.Sanz, F.Heitmeir (2006) *Laser-optical investigation of stator-rotor interaction in a transonic turbine,* Proc. 12 th International Symposium on Flow Visualization, September 10-14, 2006, German Aerospace Center (DLR), Göttingen, Germany

12TH INTERNATIONAL SYMPOSIUM ON FLOW VISUALIZATION
September 10-14, 2006, German Aerospace Center (DLR), Göttingen, Germany

LASER-OPTICAL INVESTIGATION OF STATOR-ROTOR INTERACTION IN A TRANSONIC TURBINE

Jakob WOISETSCHLÄGER[*], Rene PECNIK[*], Emil GÖTTLICH[*], Oliver SCHENNACH[*], Andreas MARN[*], Wolfgang SANZ[*], Franz HEITMEIR[*]

**[*]Institute for Thermal Turbomachinery and Machine Dynamics,
Graz University of Technology, Inffeldgasse 25A, A – 8010 Graz, Austria
jakob.woisetschlaeger@tugraz.at , www.ttm.tugraz.at**

Keywords: *Particle Image Velocimetry, turbomachinery, transonic flow, blade row interaction, computational fluid dynamics*

ABSTRACT

This paper presents research in a highly-loaded cold-flow transonic turbine under continuous and engine like conditions. Special focus was placed on blade row interaction at app. 10600 rpm. While the first step was the investigation of a single stage machine (stator-rotor), the second step extended the test rig to a one and a half stage configuration (stator-rotor-stator) with focus on "clocking" effects between the first and second stator vanes. Measurements were carried out in the transonic test turbine at Graz University of Technology using Particle-Image-Velocimetry and Laser-Doppler-Anemometry to investigate the influence of shock reflections by the rotor blades on vortex shedding from the trailing edges of the stator and rotor blades. The main results of these experiments are discussed and compared to numerical simulations focusing on the visualization of both experimental and numerical results.

1 INTRODUCTION

The trend for industrial gas turbines is towards higher efficiency at constant and possibly decreasing costs per kW shaft power. Advanced 3-D aerodynamic design and higher cycle temperatures tackle the objective of higher efficiency. In order to reduced costs it is advantageous to reduce the number of stages, thus resulting in high-pressure (HP) ratios and transonic conditions for the remaining stages. Shock systems and wakes generated by stator and rotor blades cause unsteadiness in the flow through turbomachines, related to the relative motion between rotor and stator.

In multistage turbines this mixing of stator and rotor wakes from sequent stages results in a complex situation for numerical flow predictions. In subsonic flows, a number of researchers investigated these effects by measurements and numerical simulations to better understand the unsteady flow phenomena involved [1-5]. With respect to HP stages operating under transonic conditions the problem is even more complicated due to the shock waves generated by the stator and rotor blades impacting on the following cascade of blades [6,7]. To find the appropriate position for the second stator row in such machines, a detailed investigation behind a transonic single-stage turbine at DLR, Germany, was performed [8,9] suggesting two axial positions behind the rotor where the shock strength is reduced and the next stator blades should be placed.

This basic idea of clocking (also known as indexing) is related to the overall improvement of efficiency by varying the circumferential and/or the axial position of adjacent stator or rotor blades. Usually the 2nd downstream stator is rotated with respect to the 1st stator (nozzle ring), while the largest efficiency increase is achieved with equal stator blade counts in both stators.

To investigate the unsteady but periodic flow phenomena in HP turbines and compressors a number of authors use different laser-optical techniques, e.g. Particle-Image-Velocimetry (PIV, [10-13]) or Laser-Doppler-Velocimetry (LDV, [14-17]). These techniques avoid flow blockage and are not mechanically influenced by strong pressure fluctuations.

Parallel to the recording of experimental data a number of authors developed numerical simulations for these very complex fluid flows through HP turbines [8,18-20]. These numerical codes are then validated by the experimental data, in most cases providing new insights in the complex flow physics.

2 METHODS APPLIED

2.1 Experimental Setup

The transonic test turbine of the Institute for Thermal Turbomachinery and Machine Dynamics is a continuously operating cold-flow open-circuit facility and allows the testing of turbine stages with a diameter up to 800 mm in full flow similarity (corrected speed and pressure ratio). Pressurized air is delivered to a mixing chamber by a separate 3 MW compressor station. A membrane type coupling directly transmits the turbine shaft power to a three stage radial brake compressor and measures the torque. This brake compressor delivers additional air to the air flow from the compressor station into a mixing chamber thus increasing the overall mass flow. The air temperature at turbine stage inlet can be adjusted by the compressor station coolers in a range between 40°C to 185°C. The maximum shaft speed of the test rig is limited to 11550 rpm. Detailed information on the design and operation of the facility can be found in [21].

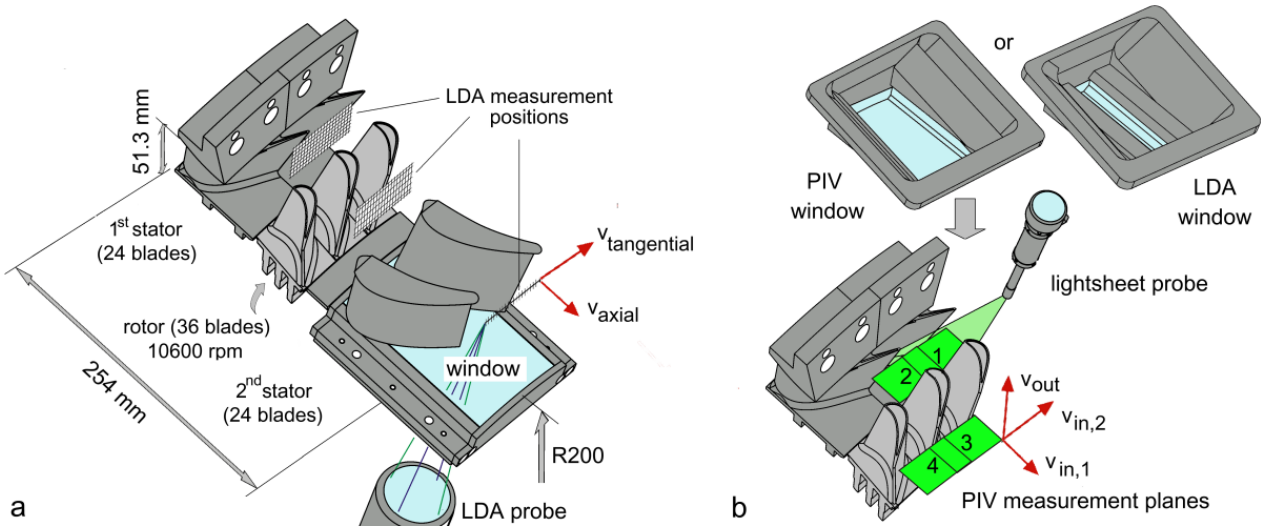

Fig. 1 – Test section. a) shows the stator-rotor-stator section of the transonic turbine with the measurement grid for Laser-Doppler-Anemometry (LDA). b) gives the stator-rotor section with planes 1- 4 in which in-plane (in) and out-of-plane (out) components of the velocity v were recorded by Particle-Image-Velocimetry (PIV).

The test section of the transonic turbine is given in Fig.1a . 24 stator blades are followed by 36 rotor blades and 24 stator vanes in the 2nd stator. A convergent-divergent flow path accelerates the flow to supersonic velocity in the 1st stator region. The pressure ratio over the first stage (stator-rotor) was 3.5, the pressure ratio over all 1 ½ stages 4.27, respectively. Rotational speed was 10600 rpm, inlet temperature about 130-140°C.

For the Laser-Doppler-Anemometry (LDA) optical access to the 1st stator - rotor section was realized through a small plane-parallel glass window (Fig.1b). The Particle-Image-Velocimetry (PIV) used a plane-concave window instead (both were made of HERASIL high-temperature quartz glass). Downstream the 2nd stator a convex-concave window of 9 mm thickness and 140x90mm surface dimension was used and is shown in Fig.1a. Anti-reflection coating was applied to all windows.

2.2 Laser Optical Measurement Techniques

For velocity recording a stereoscopic PIV (DANTEC FlowMap 1500) together with two DANTEC 80C60 HiSense cameras (1280x1024 pixel) and a NEW WAVE Gemini double cavity Nd:YAG laser (120 mJ/ pulse) were used. A special light-sheet optics consisting of a spherical lens (600 mm focal length), a cylindrical lens (−10 mm focal length), and a prism was used to illuminate the seeding particles in plane sections of the flow. For each camera the double images from one PIV recording were evaluated using a cross-correlation technique and an interrogation area size 64x64 pixel with 50% overlap. Finally, a range validation, a correlation peak ratio validation, and a moving average validation were applied to reject invalid vectors [11]. The time between the two pulses was 1 µs downstream of the 1st stator, 1.5 µs downstream the rotor. Fig. 1b shows planes 1-4 in which the in-plane and out-of-plane components of the velocity were recorded by PIV. These components were needed to derive the axial, circumferential and radial velocity components. Calibration was performed using a special calibration target, a 100x100 mm white plate with a square grid of black dots, dot spacing 2.5 mm, dot size 1.5 mm, provided by DANTEC. Thus target was placed in the position of the light-sheet [11,13]. Finally, a map of 39x31 vectors was recorded for planes 1 and 2, a 39x29 vector map for planes 3 and 4. Planes 1 and 2 were 47.5x37.5mm in size, planes 3 and 4 were 47.5x35mm, respectively, all with 1.25 mm step size.

A second set of velocity data was recorded by a two-component LDA-system (DANTEC FiberFlow with two BSA processors) using a 6W argon-ion laser (COHERENT) operated at approximately 400 mW in all lines, with the velocity component recorded in axial direction and the other component in circumferential direction (see Fig.1a). The focal length used was 400mm, the beam diameter 2.2mm [13]. The spacing of the measurement grid was approximately 3mm in circumferential direction (Fig.1a).

To allow analysis of the data related to the angular position of the rotor, one key-phasor reference signal and 12 TTL overspeed-tachometer signals per revolution were provided by the monitoring system of the turbine to trigger the data sampling (uncertainty: blade pitch/300, a phase delay depending on speed was accounted for). The sampling frequency by the BSA processor leads to an angular resolution of 0.01° (record interval 0,17 µs) compared to the 0.3° uncertainty caused by the trigger system. In all LDA measurement positions about 80000 velocity bursts were recorded and mapped into 40 time intervals within one blade passing period (app. 0.16 ms, corresponding to the movement of the rotor blades for one 10° section or one rotor blade pitch). Using a linear regression method presented in [22] the velocities were ensemble averaged to provide velocities and turbulence levels for each of the 40 rotor-stator positions. For the PIV six angular rotor-stator positions were

investigated for planes 1 to 4, using 180 sets of PIV double-images for the averaging process in each rotor stator-position. Both stators were mounted on rotatable rings. All 20 circumferential positions traversed with the LDA and the 4 planes recorded with the PIV were adjusted by moving the stators rather than moving the LDA probe or the PIV cameras.

The stator blades, the rotor blades and the endwalls were covered with a high-temperature flat black paint to reduce surface reflections. Droplets of DEHS oil (Di-Ethyl-Hexyl-Sebacin-Esther) with a nominal diameter of 0.3 µm were added by PALLAS AGF 5.0D seeding generator app. 0.3 m upstream of the 1st stator row as seeding material for the measurements. The fringe modulation of the burst signals was used to reduce the influence of too large droplets (BSA quality factor).

2.3 Computational Fluid Dynamics (CFD) and Data Visualization

Beside the laser optical measurements, a numerical simulation was done to gain understanding of the flow phenomena in the discussed test facility and further to validate the numerical scheme.

The Computational Fluid Dynamics (CFD) computations were performed using the in-house Navier-Stokes code LINARS, developed at the Institute for Thermal Turbomachinery and Machine Dynamics at Graz University of Technology [19, 23]. The compressible Reynolds/Favre-averaged Navier-Stokes (RANS) equations are solved in conservative form by means of a fully-implicit time-marching finite-volume method on structured curvilinear grids in multiblock alignment (see Fig.2). To cope with unequal pitch ratios, the code uses phase-lagged boundary conditions at geometrical periodic boundaries and hence only one passage each blade row was simulated with app. 2,000,000 cells. The geometrical details of the turbine stage containing the fillets and the rotor tip clearance were modelled as well. These fillets were formed at the 1st and 2nd stator hub, tip and the rotor hub and minimize the strains in the real machine. An O-type block encloses the blade, containing also the inlet section. A thin block is arranged close to the wall faces, which covers the entire wall domain of the blades. An H-type grid block was used to model the outlet area behind each blade. All together 27 blocks formed the computational domain.

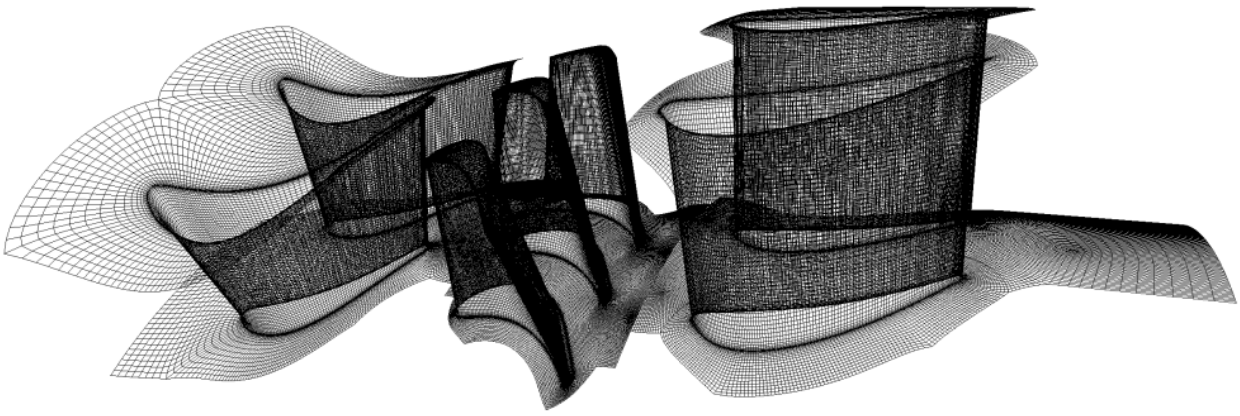

Fig. 2 – Computational domain. The picture shows the surface mesh of the computational grid used for CFD. The fillets between blades-hub and blades-outer casing and the rotor blade clearance are meshed to match the geometrical details of the test turbine facility. Approximately 5,000,000 cells were used for post-processing with two stator passages and three rotor passages.

To save computational time and memory pressure gradient wall-functions based on the law-of-the-wall formulation by Spalding were used. The turbulence closure was done using the turbulence model of Spalart and Allmaras [26]. To achieve high order accuracy a total variation-diminishing (TVD) scheme with third-order interpolation was applied for the spatial discretization and a second order accurate Newton-Raphson procedure was applied for the integration in time. One blade passing period was calculated with 480 time steps.

Using the numerical and experimental data a final post processing is essential, since the mutual comparison facilitates understanding of the complex and unsteady flow phenomena in this type of machines. Therefore, beside commercial software for data visualization own software has been developed at the Institute during the last years.

For post-processing a separate flow visualization tool was developed. This tool enables the visualization of steady as well as unsteady numerical data on structured grids. The OpenGL library was used to have access to a fast image generator to produce any desired view into the flow. It works in conjunction with a comfortable Graphical User Interface (GUI) programmed in C++. This post-processor uses a fast "marching cube" algorithm to extract iso-surfaces, draws contour plots or isolines on index surfaces, facilitates transparent shading of surfaces, as well as, texture mapping on surfaces with bitmaps. Further the post-processor facilitates different lightning models and the ability to define arbitrary trajectories to “fly” through datasets.

3 RESULTS AND DISCUSSION

3.1 Stator-Rotor Interaction

First investigations [13,16,19] using LDA, PIV and CFD techniques focused on the interaction of the 1st stator shock and wake system with the following rotor blades. A flow visualization based on all results is presented in Fig.3, including velocity data recorded by LDA, entropy as calculated by the CFD simulation and isolines of pressure gradients (CFD) visualizing the shock system, similar to the way a Schlieren technique does. Fig.3 presents the flow phenomena within one blade passing period of approximately 0.16 ms (6360 Hz) in eight successive frames.

Within the 1st stator the flow accelerates to a Mach number of about 1.5, causing a pronounced shock system at the suction side of the stator blades close to the trailing edges. This shock is visible in the velocity data and by means of the pressure gradients in the CFD simulation (encircled in Fig.3b). The strength and position of this shock varies slightly over the height, due to the influence of secondary flow structures close to the tip of the blade, e.g. passage vortex or tip vortex. Bypassing rotor blades reflect this shock system (marked in Fig.3c). In Figs. 3d and 3h these reflected shocks waves interact with the suction side boundary layer on odd (Fig.3h) and even (Fig.3d) numbered stator blades due to the 2:3 ratio between stator and rotor blades. Additionally, parts of the shock waves are reflected a second time, with the second reflection at the pressure side of the rotor blades (encircled in Fig.3c). This second reflection then influences the suction side boundary layer of the rotor blades.

Behind the turbine blades shedding boundary layer material forms a vortex street, or wake. These wakes forming behind the stator and rotor blades are also visible in Fig.3 in terms of relative entropy from the CFD results. Since the vortices in the wake move with lower velocity than the main flow, they are clearly visible in the velocity data obtained by LDA (circles in Fig.3f). When transported through the rotor blade channel, the stator wakes are chopped by the rotor blades into single segments. These segments consist of clock-wise and counter-clock-wise rotating vortices,

finally superimposed to the vortices shedding from the rotor blades. As already predicted by [9], vortices rotating in opposite direction increase their strength and widen the wake (marked in Fig.3g). This effect and reflected shocks modulate the vortex shedding from the rotor blades.

In Fig. 3a passage vortices behind the rotor blades are marked. These upper passage vortices, evoked by the turning of the fluid in the blade passages, migrate downwards due the strong tip leakage flow (from the pressure side to suction side over the blade tip).

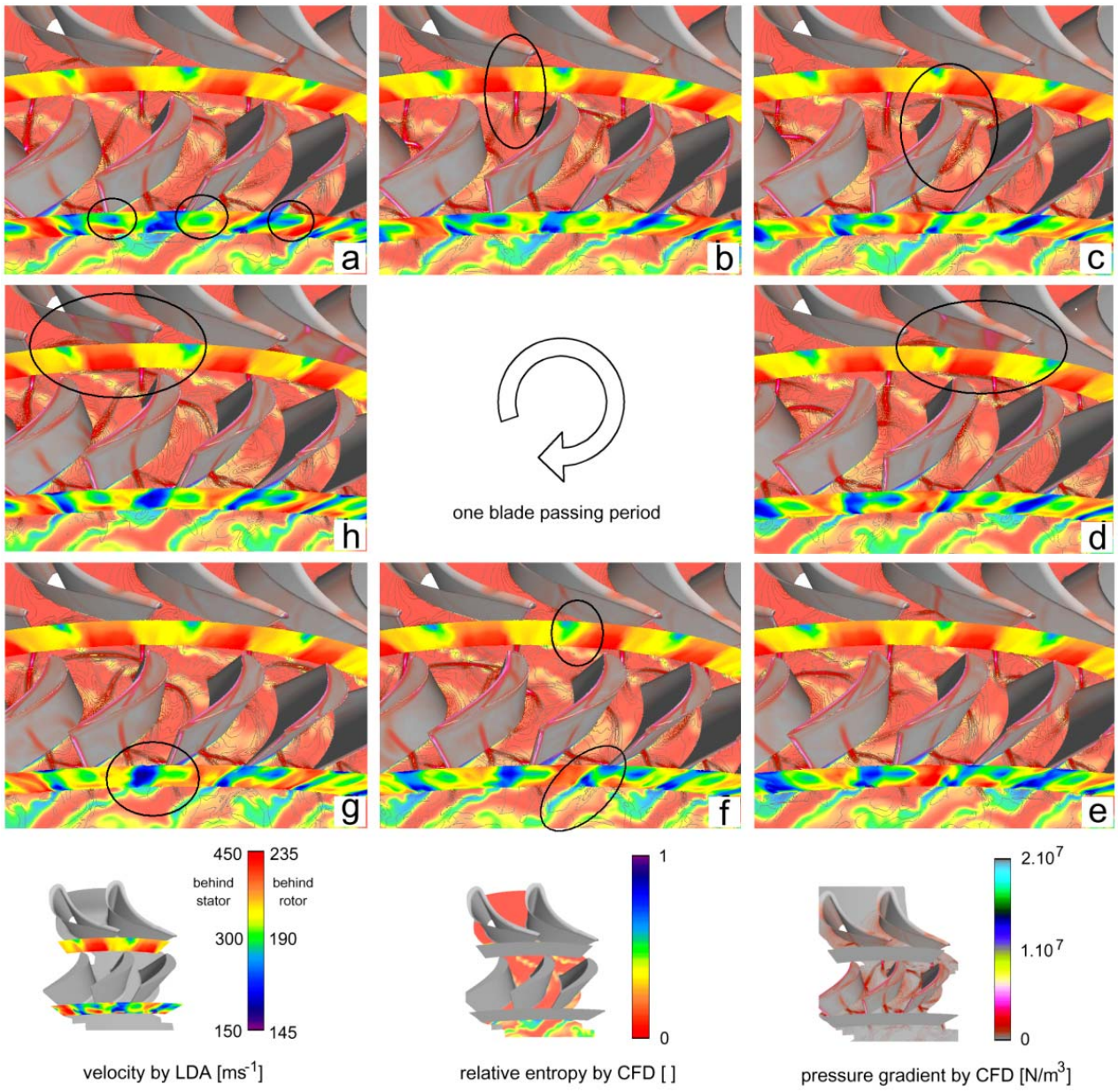

Fig. 3 Stator-Rotor interaction in a transonic turbine stage. Measurement data recorded by Laser Doppler Anemometry (LDA) are superimposed to the relative entropy and the pressure gradient obtained by Computational Fluid Dynamics (CFD). The eight pictures a) – h) present one blade passing period. Marked regions are explained in the text.

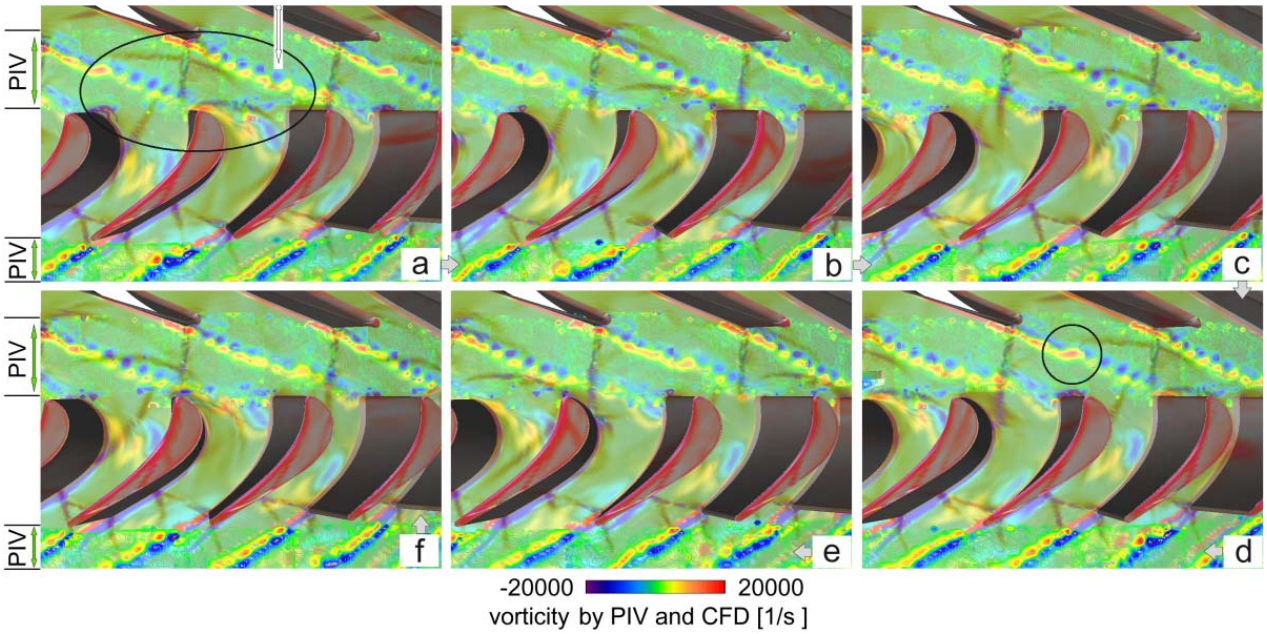

Fig. 4 – Triggered vortex shedding. In the stator-rotor gap and behind the rotor blades vorticity isolines recorded by Particle Image Velocimetry (PIV) are superimposed to results obtained by Computational Fluid Dynamics (CFD, shaded full field data). Regions marked by circles are explained in the text. The six frames present one blade passing period.

3.2 Triggered Vortex Shedding

All effects described in the previous chapter can also be studied in Fig.4 in terms of vorticity recorded by PIV and calculated by CFD. In this figure the PIV data are presented as isolines in the sections marked, superimposed to the results obtained by CFD (shaded). Additionally, the shock waves are visualized by brownish contours of pressure gradient (CFD).

In Fig.4a two shock waves reflected by two bypassing rotor blades are marked. At 10600 rpm these reflections move towards the suction side of the stator blades, slightly delayed to each other (at other speeds these shockwaves reach the stator at the same time [11]). When the first shock wave hits the suction side of the stator blade in Fig.4b, the boundary layer shedding at the trailing edge is first disrupted and then shedding of a very pronounced vortex is enforced. This vortex is marked in Fig.4d. Half a blade passing period later vortex shedding from this stator blade is back to normal (Figs.4f,a). Due to this interaction between the shock waves and the boundary layer, the vortex shedding is in phase with the bypassing rotor blades. A first numerical prediction of this effect was given by [25]. It must be kept in mind that for each of the six rotor-stator positions investigated by PIV (isolines in Figs.4a-f), at least 180 instantaneous vector fields were averaged. In the subsonic regime, with the lack of this triggering mechanisms, the phase of the vortex shedding is more or less stochastically in relation to the laser light pulses used for PIV recording, so that no separate vortices are then visible in the averaged result [24].

Caused by the second reflection of the shock wave at the pressure side of the rotor blades (Fig.3c) and its influence on the suction side boundary layer of the rotor blades, vortex shedding from the rotor blades is also modulated by the blade passing. Additionally, vortices shedding from the pressure side of the rotor blade are stronger and more pronounced than vortices from the suction side, due to the thinner boundary layer on the pressure side (see Figs.4a-f).

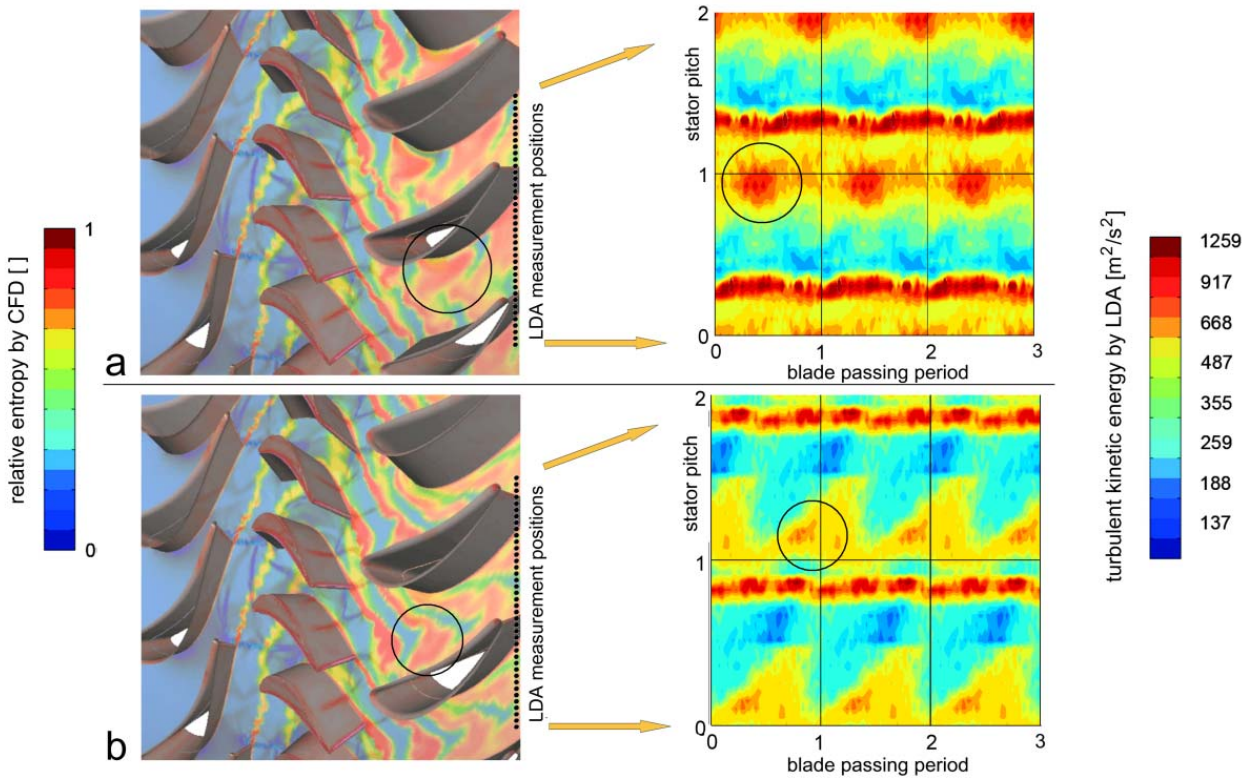

Fig. 5 – The clocking of stator blades (positions a, b) is discussed by the relative entropy calculated by Computational Fluid Dynamics (CFD) and the turbulent kinetic energy recorded by Laser Doppler Anemometry (LDA).

3.3 Clocking of Stator Blades

The information discussed in the previous sections is of relevance to the engineer when clocking is concerned. Fig.5 presents two different angular positions for the 2nd stator row relative to the 1st stator row (clocking positions a and b). Detailed measurements of 10 different clocking positions [17] indicated that for the mid-section flow, clocking results in a ± 1.6% variation in efficiency, with an efficiency maximum in position b in Fig.5 and a minimum in position a.

By the wake-wake interaction between the 1st stator wake and the rotor wake large vortical structures are produced (indicated by circles in Fig.5). In clocking position a, these structures then move through the channel of the 2nd stator and cause strong variations in turbulent kinetic energy and flow angle, negatively affecting efficiency. At the right side of Fig.5, the turbulent kinetic energy recorded by LDA is presented as space-time plot. Time is given in terms of blade passing period along the abscissa and space in terms of measurement positions along the ordinate (two blade pitches). In such a 2:3 diagram the two stator wakes show up as horizontal structures, while the influence from the rotor blades appear 45° inclined.

In Fig.5 position b the chopped wake of the 1st stator blade passes the 2nd stator blade close to its pressure side, with minimum influence on the suction side boundary layer. Additionally, the impingement of shock waves from the rotor exit at the 2nd stator is less pronounced in position b. This is due to the fact that the shock system forming at the rotor blade exit is also modulated by the bypassing 1st stator wakes (see Figs.4a-f) and the axial distance between rotor and 2nd stator meets the needs.

The spanwise total-to-total efficiency indicated that especially close to the tip the positive effect of clocking diminishes due to the strong influence of secondary flow structures. This, and an appropriately tuned blade shape will be objective of further research.

4 SUMMARY

Operating under transonic conditions, high-pressure turbines show complex flow physics mainly due to the shock systems generated by stator and rotor blades. These shocks have a strong tendency to trigger certain flow phenomena, e.g. vortex shedding from the trailing edges of the turbine blades. Superimposed in phase these effects might add up over the single stages. Proper positioning of the second stator blades will decrease the strength of this interference. Additionally, secondary flow phenomena like passage vortices and tip vortices alter these phenomena over the blade height, therefore a full three-dimensional flow design is needed.

ACKNOWLEDGEMENTS

This work was made possible by the Austrian Science Fund (FWF) within the grants P16521-N07 “Experimental Investigation of the Stator-Rotor-Stator Interaction in a Transonic Turbine”, Y57-TEC “Non-intrusive Measurement of Turbulence in Turbomachinery” and P16761 “Steady and Unsteady Transition Modelling”. The support of Dr. H. P. Pirker in the operation of the compressor station is also gratefully acknowledged. Graz University of Technology is member of the thematic network “PIV-NET 2” funded by the European Union.

REFERENCES

1. Huber FW, Johnson PD, Sharma OP, Staubach JB and Gaddis SW, Performance improvement through indexing of turbine airfoils: Part 1 – experimental investigation, *ASME J Turbomachinery* , Vol. 118, pp 630-635, 1996.
2. Gombert R and Höhn W, Unsteady aerodynamical blade row interaction in a new multistage research turbine – Part 1: Experimental Investigation, *Proceedings of the ASME TURBO EXPO 2001*, New Orleans, USA, ASME paper 2001-GT-0306, 2001.
3. Reinmöller U, Stephan B, Schmidt S and Niehuis R , Clocking effects in a 1,5 stage axial turbine – steady and unsteady experimental investigations supported by numerical simulations, *ASME J Turbomachinery,* Vol. 124, pp 52-60, 2002.
4. Arnone A, Marconcini M, Pacciani R, Schipani C. and Spano E, Numerical investigation of airfoil clocking in a three-stage low-pressure turbine, *ASME J Turbomachinery,* Vol. 124, pp 61-68, 2002.
5. Miller RJ, Moss RW, Ainsworth RW and Horwood CK, Time-resolved vane-rotor interaction in a high-pressure turbine stage, *ASME J. Turbomachinery,* Vol. 125, pp 1-13, 2003.
6. Jennions IK and Adamczyk JJ Evaluation of the interaction losses in a transonic turbine HP rotor / LP vane Configuration, *ASME J Turbomachinery,* Vol. 119, pp 69-76, 1997.
7. Haldeman CW, Dunn MG, Barter JW, Green BR and Bergholz RF, Experimental Investigation of Vane Clocking in a One and ½ Stage High Pressure Turbine, *Proceedings of the ASME TURBO EXPO 2004*, Vienna, Austria, ASME Paper No. 2004-GT-53477, 2004.
8. Tiedemann M and Kost F, Some aspects of wake-wake interactions regarding turbine stator clocking, *ASME J Turbomachinery*, Vol. 123, pp 526-533, 2001.
9. Hummel F, Wake-wake interaction and its potential for clocking in a transonic high-pressure turbine, *ASME J Turbomachinery*, Vol 124, pp 69-76, 2002.

10. Wernet MP, Development of digital particle image velocimetry for use in turbomachinery, *Exp Fluids*, Vol. 28, pp 97-115, 2000.
11. Lang H, Mørck T and Woisetschläger J, Stereoscopic particle image velocimetry in a transonic turbine, *Exp.Fluids*, Vol. 32, pp700-709, 2002.
12. Liu B, Yu X, Liu H, Jiang H, Yuan H and Xu Y, Application of SPIV in turbomachinery, *Exp. Fluids*, Vol. 40, pp 621-642, 2006.
13. Göttlich E, Woisetschläger J, Pieringer P, Hampel B and Heitmeir F, Investigation of vortex shedding and wake-wake interaction in a transonic turbine stage using Laser-Velocimetry and Particle-Image-velocimetry, *ASME J Turbomachinery*, Vol. 128, pp 178-187, 2006.
14. Zaccaria MA and Lakshminarayana, Unsteady flow field due to nozzle wake interaction with the rotor in a axial flow turbine: part 1 – rotor passage flow field, *ASME J Turbomachinery*, Vol. 119, pp 201-213, 1997.
15. Ibaraki S, Matsuo T, Kuma H, Sumida K and Suita T, Aerodynamics of a transonic centrifugal compressor impeller, *ASME J Turbomachinery*, Vol 125, pp 346-351, 2003.
16. Göttlich E, Neumayer F, Woisetschläger J, Sanz W and Heitmeir F, Investigation of stator-rotor interaction in a transonic turbine stage using Laser Doppler Velocimetry and pneumatic probes, *ASME J Turbomachinery*, Vol. 126, pp 297-305, 2004.
17. O. Schennach, J. Woisetschläger, A. Fuchs, E. Göttlich, A. Marn, R. Pecnik, Experimental investigations of clocking in a one and a half stage transonic turbine using Laser-Doppler-Velocimetry and a fast response aerodynamics pressure probe, *Proceedings of the ASME TURBO EXPO 2006*, Barcelona, Spain, paper GT2006-90264, 2006, accepted for the *ASME J Turbomachinery.*
18. Michellasi V, Giangiacorno P, Martelli F, Dénos R and Paniagua G, Steady three-dimensional simulation of a transonic axial turbine stage, *Proceedings of the ASME TURBO EXPO 2001*, New Orleans, USA, paper 2001-GT-0174, 2001.
19. Pecnik R, Pieringer P and Sanz W, Numerical investigation of the secondary flow through a transonic turbine stage using various turbulence closures, *Proceedings of the ASME TURBO EXPO 2005*, Reno, USA, paper GT2005-68754, 2005.
20. Green BR, Barter JW, Haldeman CW and Dunn MG, Averaged and time-dependent aerodynamics of a high pressure turbine blade tip cavity and stationary shroud: comparison of computational and experimental results, *ASME J Turbomachinery*, Vol. 127, pp 736-746, 2005.
21. Neumayer F, Kulhanek G, Pirker H P, Jericha H, Seyr A and Sanz W , Operational Behavior of a Complex Transonic Test Turbine Facility, *Proceedings of the ASME TURBO EXPO 2001*, New Orleans, USA, ASME paper No. 2001-GT-489, 2001.
22. Glas W, Forstner M, Kuhn K and Jaberg H, Smoothing and statistical evaluation of Laser-Doppler-Velocimetry data of turbulent flows in rotating and reciprocating machinery, *Exp. Fluids*, Vol. 29, pp 411-417, 2000.
23. Pieringer P, Göttlich E, Woisetschläger J, Sanz, W and Heitmeir F, Numerical Investigation of the Unsteady Flow through a Transonic Turbine Stage Using an Innovative Flow Solver, Proceedings 6th European Conference on Turbomachinery, Lille, France, pp. 339–352, 2005.
24. Woisetschläger J, Mayrhofer N, Hampel B, Lang H and Sanz W, Laser-optical investigation of turbine wake flows, *Exp. Fluids*, Vol. 34, pp 371-378, 2003.
25. Sondak DL and Dorney DJ, Simulation of vortex shedding in a turbine stage, *ASME J Turbomachinery*, Vol.123, pp 526-533, 1999.
26. Spalart PR and Allmaras SR, A one equation turbulence model for aerodynamic flows, *La Recherce Aerospatiale*, No.1, pp 5-21, 1994.